NUKLEONIKA 2007;52(4):153–158

ORIGINAL PAPER

Effect of scattered radiation in the total body irradiation technique: evaluation of the spoiler and wall dose component in the depthdose distribution

Tomasz Piotrowski, Karolina Adamska, Julian Malicki

Abstract. To determine the additional dose in layers of the body close to the skin during total body irradiation (TBI), due to radiation scattered off the treatment room walls and behind plexiglass spoilers applied to improve dose uniformity within the irradiated body. Large-field 6, 15 and 25 MV photon beams were generated by a Saturn 43 medical accelerator. A solid 30 × 30 × 30 cm^3 PMMA (polymethylmethacrylate) phantom was used to represent radiation scattered from the body of the patient. Dose distributions were measured by a Farmer ionization chamber. The dose component arising from the spoiler was measured 5 mm below the phantom surface, over distances of 5–100 cm between the spoiler and the phantom surface. To measure the contribution of backscattered radiation from the walls, a small lead block was placed between the source and detector. Measurements were carried out in air with the PMMA phantom removed, to eliminate radiation backscattered from the phantom. As measured behind the spoiler, attenuation of the primary photon beam by the spoiler itself was by 8, 5 and 3% for 6, 15 and 25 MV beams, respectively. The highest dose contribution from the spoiler arose at 10 cm separation between the phantom surface and the spoiler. Assessed at a depth of 5 mm in the phantom, at spoiler-phantom separation of 10 cm, relative to case without spoiler and with wall backscatter subtracted, the dose enhancement due to the spoiler was by 8, 13 and 20% at beam energies 6, 15 and 25 MV, respectively. In these measurements, the distance between the source and the phantom surface was 300 cm and that between the source and the spoiler – 290 cm. The dose contributions due to radiation backscattered from the walls, relative to the case without any wall backscatter, estimated over the distal side of the phantom at a distance of 20 cm between the wall and that side of the phantom, were 5, 6 and 8% at beam energies 6, 15 and 25 MV, respectively. The use of a spoiler enhanced the dose in regions close to the phantom surface, compensating for the dose decrease over that area due to build-up effect. Radiation backscattered from the wall enhanced the dose in regions close to the phantom surface facing the wall.

Key words: total body irradiation (TBI) • scattered radiation • leukaemia

T. Piotrowski✉
Medical Physics Dept, Great Poland Cancer Centre,
15 Garbary Str., 61-868 Poznań, Poland,
Tel.: +48 61 8850 553, Fax: +48 61 8850 550,
E-mail: piotrowski.tomasz@gmail.com
and Department of Electroradiology,
University of Medical Sciences,
15 Garbary Str., 61-868 Poznań, Poland

K. Adamska
Medical Physics Dept, Great Poland Cancer Centre,
15 Garbary Str., 61-868 Poznań, Poland

J. Malicki
Medical Physics Dept, Great Poland Cancer Centre,
15 Garbary Str., 61-868 Poznań, Poland
and Department of Electroradiology,
University of Medical Sciences,
15 Garbary Str., 61-868 Poznań, Poland
and Medical Physics Department,
School of Physics, University of Poznań,
85 Umultowska Str., 61-614 Poznań, Poland

Received: 3 January 2007
Accepted: 19 July 2007

Introduction

Total body irradiation (TBI) is a method of patient treatment prior to bone marrow transplantation in cases of acute lymphoblastic leukaemia (ALL), acute myeloid leukaemia (AML) or other disseminated malignancies [2, 4, 14]. A major problem in TBI is to achieve a reasonably homogeneous distribution dose throughout the body of the patient. Usually, this requires the application of large irradiation fields, of approximately 50 × 200 cm, achievable by selecting extended source-to-skin distances (SSD) of up to 300 cm, against the normal SSD = 100 cm [3, 5, 10]. Such extended SSD values may be difficult to obtain as the dimensions of the treatment room are usually smaller than those required in the TBI procedures [8, 17].

The use of megavoltage photon beams linear from accelerator leads to a more homogeneous dose distribution in the patient's body, in comparison to that obtained using cobalt-60 beams. However, as a result of the application of megavoltage beams, the dose in the layers of the body close to the skin decreases more steeply and more radiation becomes backscattered from the walls, additionally exposing the patient [9, 20, 22–25]. Consequently, layers of the body close to the skin of the side of the patient facing the beam may not receive enough exposure while the side of the patient facing the wall may become over-exposed due to backscattered radiation. These side effects can be avoided or diminished by placing a plexiglass spoiler between the patient's body and the source, and by allowing adequate space distances between the body of the patient and the walls of the treatment room [3, 7, 11, 16]. From the clinical point of view, skin is not a dose limiting factor during total body irradiation, because doses absorbed in the skin do not exceed the tolerance value. However, in the process of radiotherapy, eradication is required of residual neoplastic cells which may be disseminated over the whole body, including the skin [2]. Therefore, supplemental irradiation of the skin, and of layers of the body close to the skin (at depths below 0.5 cm) need to be implemented [16, 17].

The TBI technique also requires extensive quality assurance protocols involving all members of the therapeutic team, including the staff who execute the irradiation, as well as time-consuming *in vivo* and absolute dosimetry [11–13, 15, 18, 19].

The aim of this study was to establish the relationship between dose in the layers of the body close to the skin (as represented in a solid phantom at an effective measurement depth of 5 mm) due to the application of a spoiler, and to evaluate the contribution of radiation backscattered from the treatment room walls for 6, 15 and 25 MV photon beams applied at the Great Poland Cancer Centre in Poznań.

Material and methods

TBI was performed in 8 fractions over 4 consecutive days with 2 fractions per day (mornings and afternoons) and 6 h interval between. A total dose of 12.6 Gy was specified in the patient's midline in the central beam axis (CAX). During 6 fractions the patient was irradiated by lateral fields and during 2 fractions – by antero-posterior fields. Lateral field irradiation consumed less time and was more comfortable for the patients. Antero-posterior fields were used to provide a stable set-up for lung shielding. The ratio between doses delivered from lateral and antero-posterior fields was determined in order to provide a prescribed dosage fall in the lungs. Initially, TBI was carried out on the cobalt unit but was later transferred to a linear accelerator [9, 14, 15].

In this study, characteristic of the dose measured at the effective depth equal to 5 mm (representing layers of the body close to the skin) was evaluated in beams generated by a linear accelerator. A Saturn 43 (General Electric) linear accelerator was used as the source of photon beams of nominal energy 6, 15 and 25 MV. Dosimetry was performed using an Ionex 2500/3 dosimeter (Nuclear Enterprises) with a 0.6 cm^3 NE 2571 ionization chamber. All irradiations were carried out with the accelerator set to 200 monitor units.

Dose component from the spoiler, D_A

A solid PMMA 30 × 30 × 30 cm phantom, made of several layers, of density 1.06 g/cm^3, was used.

A plexiglass spoiler of 1 cm thickness was placed between the phantom and the source. The radiation scattered in the spoiler was mainly absorbed at smaller depths and increased the dose there. The spoiler attenuated intensity of primary photon beam, and the attenuation factor, depended on photon energy [11, 21]. The attenuation of the primary photon beam was determined for all investigated beams (6, 15 and 25 MV). The spoiler attenuation factor was determined using the formula:

$$S = (D_{0,d_{\mathrm{ref}}} - D_{s,d_{\mathrm{ref}}}) / D_{0,d_{\mathrm{ref}}} \quad (1)$$

where: $D_{0,d_{\mathrm{ref}}}$ and $D_{s,d_{\mathrm{ref}}}$ are doses measured with or without the spoiler, at the same reference depth (d_{ref}) in the solid phantom. The reference depth was set to 5 cm for 6 MV and to 10 cm for 15 and 25 MV, respectively.

The dose component D_A from radiation scattered in the spoiler was calculated using the following formula:

$$D_A = [D_{s,d_s}*(1 + S) - D_{0,d_s}]*100\% \quad (2)$$

where: S is the spoiler attenuation factor, and D_{s,d_s} and D_{0,d_s} are, respectively, doses measured with or without the spoiler at the depth d_s = 5 mm in the phantom, representing layers of the body close to the skin surface. Doses (D_{s,d_s}) were measured over a range of distances (x = 5÷100 cm) between the spoiler and the phantom surface, while the distance between the source and detector remained constant (SSD = 300 cm). In Fig. 1 a set-up used for the measurements of attenuation factor and D_A component is presented. The detector

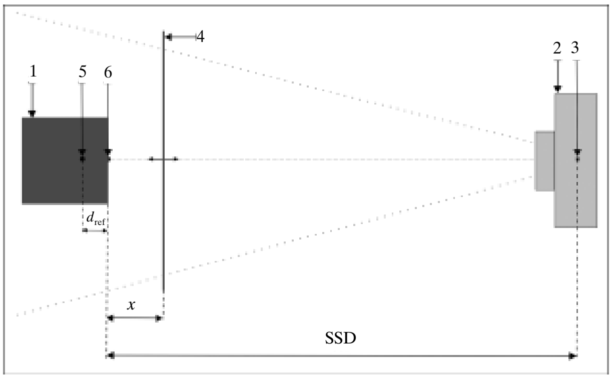

Fig. 1. The set-up used for measurements of the attenuation factor and of the D_A component (radiation scattered in the spoiler). 1 – solid phantom (30 × 30 × 30 cm); 2 – accelerator gantry in horizontal position; 3 – source; 4 – plexiglass spoiler, 5 – position of the detector during measurements of the attenuation factor (at a reference depth d_{ref}); 6 – position of the detector during measurements of D_A; SSD – source-surface distance of 300 cm (constant); d_{ref} – reference depth in the phantom (5 cm for 6 MV and 10 cm for 15 and 25 MV); x – distance between the phantom surface and the spoiler (ranging from 5 to 100 cm).

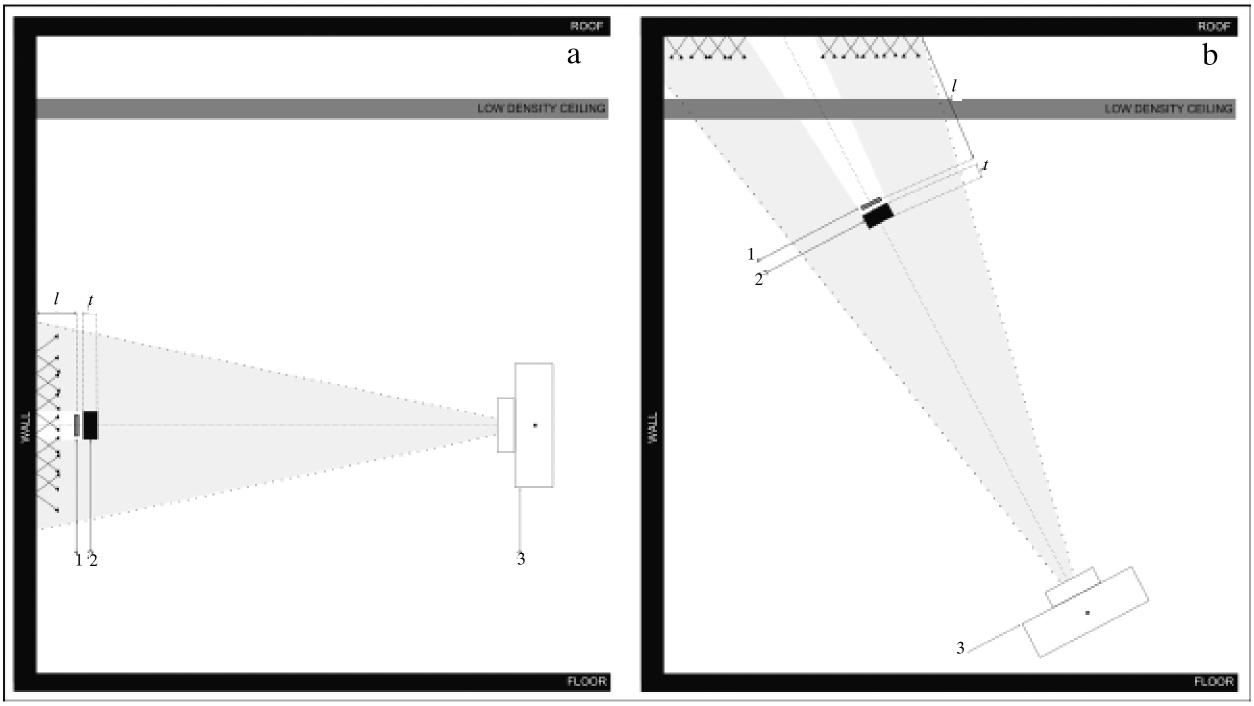

Fig. 2. The set-up used in measurements of D_B component (radiation backscattered from the walls). 1 – position of the detector (in central beam axis); 2 – lead block placed between the detector and source; 3 – gantry of the accelerator. Distances between the detector (1) and block (2) were equal in measurements shown in Figs. 2a and 2b. In Fig. 2a, the distance between the detector and wall changed from 10 cm to 100 cm. The distance between the roof and the detector presented in Fig. 2b was 250 cm (constant).

was placed at a reference depth in the solid phantom (point 5, Fig. 1). Doses were measured with or without the spoiler. The component D_A (formula 2) was measured with the detector placed on the phantom surface (point 6, Fig. 1). The spoiler position was changed from 5 to 100 cm (x, Fig. 1). In all measurements the detector was placed in the central axis of the beam.

Measurements of the dose at the depth d_s = 5 mm, representing layers of the body close to the skin surface, were carried out with the 2571 ionization chamber fitted with a 0.5 cm thick cap, fastened to the phantom surface. This constituted only partial build-up conditions for energies larger above 6 MV [1, 6, 8]. However, providing sufficient build-up would counteract the aim of the study in which doses near the surface were to be evaluated.

Dose component from the walls of the room, D_B

The primary photon beam interacted with the walls of the treatment room and generated secondary backscattered radiation which exposed the phantom from the side nearest to the wall. To measure the dose component originating from radiation backscattered in the walls, a small lead block was placed between the source and detector. The thickness of the block was 10 cm, which ensured that the intensity of the primary photons behind the block was reduced almost to zero. These measurements were carried out in air in order to avoid secondary radiation generated during measurements in the phantom. The dose component D_B from radiation backscattered from the walls was calculated using the formula:

(3) $$D_B = (D_w - D) / D*100\%$$

where: D_w and D are the doses measured with and without wall influence, respectively.

To eliminate the impact of walls on dose a special set-up was designed and built. The beam was directed towards the ceiling. The distance between the source and the reinforced roof was much greater than that between the source and wall. Moreover, an additional ceiling, made from low density material, absorbed the scattered radiation before it reached the detector. Therefore, doses measured in these conditions were assumed not to be influenced by the walls. In Fig. 2 the set-up used for measurements of the D_B component (radiation backscattered from the walls) is presented.

Results

The attenuation factors (S) of the primary photon beam in the plexiglass spoiler depended on the energy of the photon beam. No significant dependence between the attenuation factors (for the beams applied) and the distance between the phantom surface and the spoiler (x) was evident (p = 0.83 without increasing/decreasing trends). Therefore, the distance x = 10 cm and SSD = 300 cm were chosen as the representative conditions. Values measured in these conditions are presented in Table 1.

Table 1. Attenuation factors S (%) of the primary photon beam in the plexiglass spoiler measured in TBI conditions at depths of 5 cm 6 MV, and at 10 cm for 15 and 25 MV beams. SSD = 300 cm; distance between phantom's surface and the spoiler equal to 10 cm

d_{ref} (cm)	S (%)		
	6 MV	15 MV	25 MV
5	5	–	–
10	–	3	3

In Table 2 and Fig. 3 the dose components D_A in the phantom, due to the plexiglass spoiler, are presented. Doses measured with the spoiler $D_{s,d_s}(1 + S)$ were normalized to those without the spoiler D_{0,d_s}. The uncertainty of measured doses was estimated at 1%.

The dose components in the phantom coming from the walls of the treatment room D_B and their relationships with distance l between the wall and the detector for the 6, 15 and 25 MV beams are shown in Table 3 and in Fig. 4.

The uncertainties of the measured dose values were estimated using the following formula:

$$\delta q = \sqrt{\left(\left|\frac{\delta q}{\delta x}\right|\delta x\right)^2 + \ldots + \left(\left|\frac{\delta q}{\delta z}\right|\delta z\right)^2} \tag{4}$$

where: $d_x,\ldots, d_z$ are the independent and random errors, respectively: of the phantom, spoiler, and detector positions during measurements of D_A; and of block and detector positions during measurements of D_B. These uncertainties did not exceed 1%. The calibration factors for the ionization chamber, including influence of temperature and pressure changes, were taken into account.

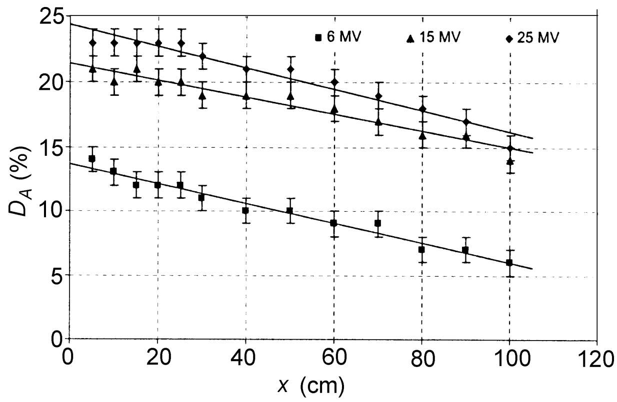

Fig. 3. Doses measured with the spoiler $D_{s,d_s}(1 + S)$ at the phantom surface D_A (%) vs. the distance x between the spoiler and phantom for 6, 15 and 25 MV beams, normalized to those without the spoiler, D_{0,d_s} = 100%. Error bars represent measurement uncertainties.

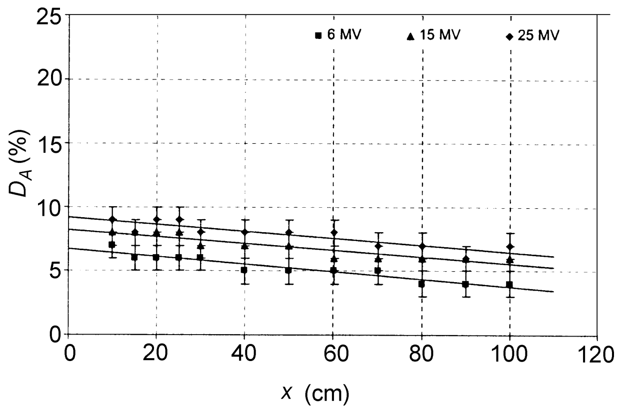

Fig. 4. Dose components D_B in the phantom arising from the walls of the treatment room vs. the distance l between the wall and the detector, for 6, 15 and 25 MV photon beams. Error bars represent uncertainties of dose determination.

Table 2. Doses measured with the spoiler $D_{s,d_s}(1 + S)$ at the phantom surface D_A (%) at distance x between the spoiler and the phantom, normalized to those without the spoiler D_{s,d_s} = 100%, for 6, 15 and 25 MV beams

x (cm)	6 MV		15 MV		25 MV	
	$D_{s,d}(1 + S)$	D_A	$D_{s,d}(1 + S)$	D_A	$D_{s,d}(1 + S)$	D_A
	(%)					
5	114	14	121	21	123	23
10	113	13	120	20	123	23
15	112	12	121	21	123	23
20	112	12	120	20	123	23
25	112	12	120	20	123	23
30	111	11	119	19	122	22
40	110	10	119	19	121	21
50	110	10	119	19	121	21
60	109	9	118	18	120	20
70	109	9	117	17	119	19
80	107	7	116	16	118	18
90	107	7	115	16	117	17
100	106	6	114	14	115	15

Table 3. The dose contribution D_B in the phantom arising from radiation backscattered for the walls of the treatment room, at distance l between the wall and the detector for 6, 15 and 25 MV photon beams. Doses measured "with walls", D_w, were normalized to those measured "without walls", D = 100%

SSD (cm)	l (cm)	6 MV		15 MV		25 MV	
		D_w	$\boldsymbol{D_B}$	D_w	$\boldsymbol{D_B}$	D_w	$\boldsymbol{D_B}$
		(%)					
340	10	107	**7**	108	**8**	109	**9**
335	15	106	**6**	108	**8**	108	**8**
330	20	106	**6**	108	**8**	109	**9**
325	25	106	**6**	108	**8**	109	**9**
320	30	106	**6**	107	**7**	108	**8**
310	40	105	**5**	107	**7**	108	**8**
300	50	105	**5**	107	**7**	108	**8**
290	60	105	**5**	106	**6**	108	**8**
280	70	105	**5**	106	**6**	107	**7**
270	80	104	**4**	106	**6**	107	**7**
260	90	104	**4**	106	**6**	106	**6**
250	100	104	**4**	106	**6**	107	**7**

Discussion

The portion of the primary photon beam attenuated by the plexiglass spoiler did not exceed 5% for 6 MV or 3% for 25 MV at their respective reference depths. This effect was not clinically relevant, because it decreased the dose rate only slightly, and thus the time of irradiation increased insignificantly, and had no impact neither on clinical results nor on the patient's comfort. This effect however, should be taken into account in calculations of treatment exposure (number of monitor units).

During interaction with primary photons, the spoiler generated scattered electrons and additional photons of energy lower than that of incident photons. Scattered electrons and low energy photons were mainly absorbed in layers of the phantom close to its surface and consequently increased the dose there. Moreover, scattered electrons play a major role in increasing the dose in layers close to the surface, for primary photons of energy 6 MV and higher. This effect is clinically important if photon beams of 6, 15 or 25 MV are used, because photons in these beams demonstrated large build-up effect, which was evident at depths of 1.2, 1.6 and 2.4 cm, respectively. In conditions of TBI these maximum dose depths are smaller than those observed during standard radiotherapy at shorter SSDs and smaller fields [8, 11]. However, this effect leads to significant dosage drop near the surface, which could result in poorer eradication of residual neoplastic cells. Measurements have shown that doses at the phantom surface were 90% for 6 MV, 78% for 15 MV and 69% for 25 MV without a spoiler and could be increased respectively by 13, 20 and 23%, if a plexiglass spoiler was placed at a distance of 10 cm from the surface of the phantom [9, 11]. These results were normalized to the maximum dose which was measured by the Farmer ionization chamber placed in the solid (plexiglass) phantom at the maximum depths for each photons energy in TBI conditions (SSD = 300 cm; field size equal to 40 × 40 cm at the isocentrum – SSD = 100 cm; accelerator gantry rotated by 90 degrees). Adding a spoiler should improve dose homogeneity throughout the whole body during photon irradiation and thus improve the process of neoplastic cell eradication.

Dose components from the walls of the room were evaluated at several distances between the phantom and wall. Larger variations in doses were apparent for beams of lower energy and were determined as lying between 4% and 7% for 6 MV and as between 7% and 9% for 25 MV photons only. This effect caused an increase of dose over the side of the patient nearest to the walls of the room, and should be taken into account.

The obtained results should lead to an improvement in the accuracy of dose delivery by taking into account the possible under- or overdosage, to be eliminated by modifying the irradiation fields or by changing the patient set-up in the treatment room.

Conclusions

1. The use of a plexiglass spoiler increased doses in the layers of the phantom close to its surface. The largest dose increase was observed at a distance of 10 cm between the phantom surface and the spoiler. At this distance, dose components were 13, 20 and 23% for 6, 15 and 25 MV photon beams, respectively.
2. Variations in dose components associated with backscattered radiation in the walls were greatest for 6 MV and least for 25 MV photons. Measured values at a distance of 20 cm between the wall and detector were 6, 8 and 9% for 6, 15 and 25 MV photon beams, respectively.

References

1. Almond PR, Biggs PJ, Coursey BM *et al*. (1999) AAPM's TG-51 protocol for clinical reference dosimetry of high-energy photon and electron beams. Med Phys 26:1847–1870
2. Barret A (1999) Total body irradiation. Rep Pract Oncol Radiother 4:47–64
3. Engler MJ (1986) A practical approach to uniform total body photon irradiation. Int J Radiat Oncol Biol Phys 12:2033–2039
4. Grinsky T, Briot E, Bridier A *et al*. (1997) Principles of total body irradiation. Rep Pract Oncol Radiother 2:33–35
5. Hui SK, Das RK, Thomadsen B *et al*. (2004) CT-based analysis of dose homogeneity in total body irradiation using lateral beam. J Appl Clin Med Phys 5:71–79
6. Kassaee A, Xiao Y, Bloch P *et al*. (2001) Doses near the surface during total-body irradiation with 15 MV X-rays. Int J Cancer 96:125–130
7. Lin JP, Chu TC, Liu MT (2001) Dose compensation of the total body irradiation therapy. Appl Radiat Isot 55:623–630

8. Litoborski M, Zwierzchowski G, Kierkowski J *et al*. (2006) Dose distribution and parameters of the linear accelerators used in Great Poland Cancer. Zeszyty Naukowe Wielkopolskiego Centrum Onkologii 3:115–311 (in Polish)
9. Malicki J (1997) Beam filter and compensators during total body irradiation on cobalt-60. Rep Pract Oncol Radiother 2:77–81
10. Malicki J (1998) Homogeneity and accuracy of the dose determination during total body irradiation. J Med Phys 23:80–81
11. Malicki J (1999) The accuracy of dose determination during total body irradiation. Strahlenther Onkol 175:492–496
12. Malicki J (2005) A career pathway for radiation therapists. Does it really exist? In regard to Kresl *et al*. "A historical perspective of the radiation oncology workforce and ongoing initiatives to impact recruitment and retention". Int J Rad Oncol Biol Phys 62:292–293
13. Malicki J, Litoborski M, Kierzkowski J *et al*. (2004) How the implementation of an *in vivo* dosimetry protocol improved the dose delivery accuracy in head and neck radiotherapy. Neoplasma 51:155–158
14. Malicki J, Wachowiak J, Kosicka G *et al*. (1996) Dose distribution and early therapeutical effects of the total body irradiation for acute leukemia patients before bone marrow transplantation. Nowotwory 46:731–736 (in Polish)
15. Nowak A, Malicki J, Wachowiak J *et al.* (2001) Comparison of doses measured by thermoluminescent and semiconductor detectors during total body irradiation at cobalt-60 and 15 MeV linear accelerator. Rep Pract Oncol Radiother 6:40
16. Planskoy B, Bedford AM, Davis FM, Tapper PD, Loverock LT (1996) Physical aspects of total-body irradiation at the Middlesex Hospital (UCL group of hospitals), London 1988–1993: I. Phantom measurements and planning methods. Phys Med Biol 41:2307–2326
17. Quast U (1997) Total body irradiation – review of treatment techniques in Europe. Radiother Oncol 9:91–106
18. Ragona R, Anglesio S, Urgesi A *et al*. (1987) Technics and dosimetry in total body irradiation with 18 MeV photons. Radiol Med (Torino) 73:438–442 (in Italian)
19. Rittmann KL (1996) Quality assurance in total body irradiation by *in vivo* dosimetry. Rep Pract Oncol Radiother 1:21–24
20. Sanchez-Nieto B, Sanchez-Doblado F, Arrans R *et al*. (1993) Backscatter correction algorithm for TBI treatment conditions. Med Dosim 18:107–111
21. Sanchez-Nieto B, Sanchez-Doblado F, Terron JA *et al*. (1997) Lateral scatter correction algorithm for percentage depth dose in a large-field photon beam. Med Dosim 22:121–125
22. Scrimger JW (1977) Radiation backscattered from high atomic number materials in high energy photon beams. Radiology 124:815–817
23. Van Dam J, Rijnders A, Vanuytsel L *et al*. (1988) Practical implications of backscatter from outside the patients on the dose distribution during total body irradiation. Radiother Oncol 13:193–201
24. Weeks KJ, Litvienko VN, Madey JM (1997) The Compton backscattering process and radiotherapy. Med Phys 24:417–423
25. Zwierzchowski G, Piotrowski T, Kosicka G *et al*. (2006) Dose distribution during total body irradiation. Zeszyty Naukowe Wielkopolskiego Centrum Onkologii 3:5–35 (in Polish)